UCRL-ID-151070

Estimating Reaction Cross Sections from Measured γ-ray Yields: The ^{238}U(n,2n) and ^{239}Pu(n,2n) Cross Sections

W. Younes

November 18, 2002

U.S. Department of Energy

Lawrence
Livermore
National
Laboratory

DISCLAIMER

This work was performed under the auspices of the U. S. Department of Energy by the University of California, Lawrence Livermore National Laboratory under Contract No. W-7405-Eng-48.

Estimating Reaction Cross Sections from Measured γ-ray Yields: the ^{235}U$(n,2n)$ and ^{239}Pu$(n,2n)$ Cross Sections

W. Younes[†]

Lawrence Livermore National Laboratory, Livermore, CA 94551

(Dated: November 18, 2002)

A procedure is presented to deduce the reaction-channel cross section from measured partial γ-ray cross sections. In its simplest form, the procedure consists in adding complementary measured and calculated contributions to produce the channel cross section. A matrix formalism is introduced to provide a rigorous framework for this approach. The formalism is illustrated using a fictitious product nucleus with a simple level scheme, and a general algorithm is presented to process any level scheme. In order to circumvent the cumbersome algebra that can arise in the matrix formalism, a more intuitive graphical procedure is introduced to obtain the same reaction cross-section estimate. The features and limitations of the method are discussed, and the technique is applied to extract the ^{235}U$(n,2n)$ and ^{239}Pu$(n,2n)$ cross sections from experimental partial γ-ray cross sections, coupled with (enhanced) Hauser-Feshbach calculations.

I. INTRODUCTION

Reaction cross sections can be estimated from measured γ-ray partial cross sections. The simplest examples of this technique have equated the reaction cross section with the measured cross section of the $2_1^+ \rightarrow 0_1^+$ transition, in the case of nuclear reactions producing an even-A nucleus. For an odd-A or odd-odd product nucleus, the reaction-channel cross section has been approximated by the sum of yields for a few transitions to the ground state [1]. In an improved approach, additional unobserved feeding of the ground state was taken into account in an even-even rotational nucleus by fitting a spin-dependent smooth function to differences in γ-ray intensities for the members of the ground state band, and extrapolating to the $J = 0$ ground state [2]. In general the observed γ-ray transitions do not carry all the de-excitation strength, and a model calculation of the unobserved contribution is necessary to supplement the experimental data and reconstruct the channel cross section. Naturally, the more complete the experimental information is, especially at the end of the γ-ray cascades, the less model-dependent and the more accurate the estimated cross section will be.

This paper presents the formalism required to combine any number of measured and calculated (e.g., using a Hauser-Feshbach code) γ-ray partial cross sections to estimate the channel cross section. The result can be formulated simply as the sum of measured partial cross sections combined with the sum of cross sections that were not measured, but are supplied instead by a model calculation. The challenges in applying this "**sum**" method consist in relying as much as possible on experimental data and taking proper account of the de-excitation strength that may be fragmented and recombined in the level scheme as the nucleus decays to its ground state. For example, $(n,2n)$ cross sections were deduced from measured ^{235}U$(n,2n\gamma)$ and ^{239}Pu$(n,2n\gamma)$ partial cross sections [3–5] that did not include the $2_1^+ \rightarrow 0_1^+$ transition because it is highly converted. The $4_1^+ \rightarrow 2_1^+$ transition was also difficult to measure, because of contamination from fission and target radioactive background. Therefore, in those cases, the $(n,2n)$ cross-section estimate relies on other partial γ-ray cross sections, and a proper accounting of all experimental data and model calculations is essential.

In section II A the **sum** method alluded to above is explained and couched in a matrix formalism to facilitate the necessary bookkeeping. The formalism is illustrated with a simple level scheme. A general algorithm is developed in section II B that is applicable to any level scheme. An alternate, graphical method is presented in section II C that may be used to generate the matrix equation for the **sum** method in a more intuitive way. Finally, the **sum** method is used to estimate the ^{235}U$(n,2n)$ cross section in section III A, and the ^{239}Pu$(n,2n)$ cross section in section III C.

[†]Electronic address: younes@llnl.gov

II. FORMALISM

The determination of a channel cross section from measured γ-ray partial cross sections assumes that the low-lying partial level scheme of the nucleus formed in that channel is known and that observed γ rays are identified, and their contribution to the de-excitation strength can be tracked to a final (ground or isomeric) state. A model calculation (e.g., from a Hauser-Feshbach code) can then be used to supply the γ-decay strength of the unobserved transitions. Of course, the calculation must provide a reasonable prediction of the cross sections.

The known partial level scheme in the residual nucleus is at the center of any procedure used to combine measured and calculated partial γ-ray cross sections into an estimate of the channel cross section. The partial level scheme consists of a set of discrete levels and branching ratios for the transitions connecting them. Consider for example the simple decay scheme in Fig. 1. Four levels are depicted, and labeled by integer indices. In this example, the transitions from level 4 to the ground-state level 1, and from level 3 to level 2 have been observed and their yields measured, while the yields for the remaining transitions, from level 4 to 2 and from level 2 to 1, have not been measured, but their branching ratios are assumed to be known. The "side-feeding" cross section of a level in this paper is defined for a given level as the population cross section of that level not accounted for by discrete γ rays decaying directly to that level in the given level scheme. Thus, the side-feeding cross section may include contributions from direct population by the reaction process, as well as contributions from γ rays not explicitly included in the level scheme (either from discrete states or a quasi-continuum of levels). Note that this definition differs from a more restrictive version often used in the literature that limits side-feeding to the contribution from the reaction process itself.

In the particular cases of the ^{235}U$(n,2n)$ and ^{239}Pu$(n,2n)$ cross sections discussed below, the side-feeding contribution was not measured, but is provided by a model calculation based on the known partial level scheme. The formalism within which these calculated side-feeding cross sections are combined with the measured transition yields to produce the channel cross section is discussed in the sections that follow, using the level scheme in Fig. 1 as an example.

A Matrix Method

The problem of converting the level scheme represented in Fig. 1 into more practical algebraic expressions lends itself naturally to a matrix approach. For convenience, we define the following sums:

$$\begin{aligned} S_{\rm obs}^{\rm (expt)} &\equiv \text{sum of experimental cross sections for a set of non-coincident, observed } \gamma \text{ rays} \\ S_{\rm obs}^{\rm (calc)} &\equiv \text{sum of calculated cross sections for the same set of non-coincident, observed } \gamma \text{ rays} \\ S_{\rm unobs}^{\rm (calc)} &\equiv \text{sum of calculated cross sections for a set of non-coincident } \gamma \text{ rays and side-feeding} \\ &\quad \text{cross sections not observed in the experiment, and complementary to } S_{\rm obs}^{\rm (calc)} \end{aligned}$$

In the context of this paper, "non-coincident" means a given excited nucleus cannot decay through more than one of the γ rays included in the sum (i.e., no "double counting" of the decay strength). The word "complementary" in the definition of $S_{\rm unobs}^{\rm (calc)}$ simply means that the calculated reaction cross section, $\sigma_R^{\rm (calc)}$, can be written

$$\sigma_R^{\rm (calc)} = S_{\rm obs}^{\rm (calc)} + S_{\rm unobs}^{\rm (calc)}. \tag{II.1}$$

With these definitions, the **sum** method amounts to writing an estimate σ_R for the cross section, with experimental cross sections replacing calculated ones in Eq. II.1:

$$\sigma_R = S_{\rm obs}^{\rm (expt)} + S_{\rm unobs}^{\rm (calc)}. \tag{II.2}$$

This simple equation belies the difficult task of identifying a set of measured and calculated γ-ray and side-feeding contributions that are non-coincident (so that no double-counting of the de-excitation strength occurs) and complementary (so that their sums in Eq. II.2 produce a good estimate of the channel cross section). This task is more easily accomplished by casting the problem in the language of matrices.

The description of the **sum** method in terms of a matrix equation begins with the known level scheme. The branching ratio for a transition from level i to a lower level j is denoted by $\alpha_{i,j}$, and by definition

$$\sum_j \alpha_{i,j} = 1. \tag{II.3}$$

The population cross section σ_i for a level i can be obtained from the transition cross section $\sigma_{i\to j}$ from that level to any other level using the corresponding branching ratio:

$$\sigma_i = \sigma_{i\to j} / \alpha_{i,j}. \tag{II.4}$$

Alternatively, the population cross section σ_i can be obtained as the contribution from all discrete γ rays in the partial level scheme decaying directly (i.e. in one step) to that level, and the side-feeding contribution to that level (by the definition of side feeding in this paper),

$$\sigma_i = \underbrace{\sum_j \sigma_{i\to j}}_{\text{decay out}} = \underbrace{\sum_k \sigma_{k\to i}}_{\text{decay in}} + \sigma_i^{(\text{side})} \tag{II.5}$$

Eqs. II.4 and II.5 written for every state in the level scheme form a system of linear equations which can be solved for the population cross section of each level. For the four-state level scheme in Fig. 1, those equations are

$$\begin{aligned}
\sigma_1 &= \alpha_{2,1}\sigma_2 + \alpha_{4,1}\sigma_4 + \sigma_1^{(\text{side})} \\
\sigma_2 &= \alpha_{3,2}\sigma_3 + \alpha_{4,2}\sigma_4 + \sigma_2^{(\text{side})} \\
\sigma_3 &= \sigma_3^{(\text{side})} \\
\sigma_4 &= \sigma_4^{(\text{side})},
\end{aligned} \tag{II.6}$$

which can be written in a more useful matrix form:

$$\begin{pmatrix} 1 & -\alpha_{2,1} & 0 & -\alpha_{4,1} \\ 0 & 1 & -\alpha_{3,2} & -\alpha_{4,2} \\ 0 & 0 & 1 & 0 \\ 0 & 0 & 0 & 1 \end{pmatrix} \begin{pmatrix} \sigma_1 \\ \sigma_2 \\ \sigma_3 \\ \sigma_4 \end{pmatrix} = \begin{pmatrix} \sigma_1^{(\text{side})} \\ \sigma_2^{(\text{side})} \\ \sigma_3^{(\text{side})} \\ \sigma_4^{(\text{side})} \end{pmatrix}, \tag{II.7}$$

and inverted to extract the individual population cross sections σ_i. In particular, the population cross section σ_1 of the ground state is identically equal to the reaction cross section. Solving for σ_1 in this example gives

$$\begin{aligned}
\sigma_1 &= \sigma_1^{(\text{side})} + \alpha_{2,1}\sigma_2^{(\text{side})} + \alpha_{2,1}\alpha_{3,2}\sigma_3^{(\text{side})} + (\alpha_{4,1} + \alpha_{2,1}\alpha_{4,2})\sigma_4^{(\text{side})} \\
&= \sigma_1^{(\text{side})} + \sigma_2^{(\text{side})} + \sigma_3^{(\text{side})} + \sigma_4^{(\text{side})},
\end{aligned} \tag{II.8}$$

where Eq. II.3, and the assumption that $\alpha_{2,1} = \alpha_{3,2} = 1$ in Fig. 1, have been used to provide numerical values for the branching ratios. The final answer in Eq. II.8 is not surprising since it simply states that all the cross section that "enters" the level scheme in the form of side feeding eventually flows down to the ground state.

So far, the estimate of the channel cross section (i.e. Eq. II.8) has relied entirely on the model calculation. To illustrate how the **sum** method might be implemented within this matrix algebra, suppose that partial cross sections for the $4 \to 1$ and $3 \to 2$ transitions have been measured. Using Eq. II.4 and known branching ratios, the corresponding experimental population cross sections $\sigma_3^{(\text{expt})}$ and $\sigma_4^{(\text{expt})}$ for levels 3 and 4 respectively are deduced. Then the system of equations describing the flow within the level scheme becomes

$$\begin{aligned}
\sigma_1 &= \alpha_{2,1}\sigma_2 + \alpha_{4,1}\sigma_4 + \sigma_1^{(\text{side})} \\
\sigma_2 &= \alpha_{3,2}\sigma_3 + \alpha_{4,2}\sigma_4 + \sigma_2^{(\text{side})} \\
\sigma_3 &= \sigma_3^{(\text{expt})} \\
\sigma_4 &= \sigma_4^{(\text{expt})},
\end{aligned} \tag{II.9}$$

which gives the solution

$$\sigma_1 = \sigma_1^{(\text{side})} + \sigma_2^{(\text{side})} + \sigma_3^{(\text{expt})} + \sigma_4^{(\text{expt})}. \tag{II.10}$$

In this simple example, Eqs. II.8 and II.10 are very similar, with experimental cross sections, where available, replacing calculated side-feeding cross sections. This is not the case in general. In more complicated level schemes, only part of the decay from a higher-lying state in the level scheme might pass through an experimentally measured level. In that case, the solution to the corresponding set of equations would be more complicated and would involve the appropriate branching ratios explicitly. Finally, Eq. II.10 can be written in the **sum**-method form of Eq. II.2 by making the identifications:

$$\begin{aligned} S_{\text{obs}}^{(\text{expt})} &= \sigma_3^{(\text{expt})} + \sigma_4^{(\text{expt})} \\ S_{\text{unobs}}^{(\text{calc})} &= \sigma_1^{(\text{side})} + \sigma_2^{(\text{side})} \\ S_{\text{obs}}^{(\text{calc})} &\equiv \sigma_R^{(\text{calc})} - S_{\text{unobs}}^{(\text{calc})} = \sigma_3^{(\text{side})} + \sigma_4^{(\text{side})}. \end{aligned} \tag{II.11}$$

B General Algorithm

Based on the example discussed in section II A, a general matrix equation for the **sum** method can be developed that is applicable to any level scheme. After labeling the states $i = 1, \ldots, N$ in the level scheme, a matrix representation

$$A\sigma = b, \tag{II.12}$$

can be written down, where A is the coefficient matrix composed of branching ratios, σ is a vector of unknown level-population cross sections, and b is the right-hand-side vector of known (measured population or calculated side-feeding) cross sections. For each level, one of two possible types of equations can be written down. If the population cross section for the level can be determined from experiment (i.e. if the yield for one or more γ rays de-populating the level has been measured), the unknown population cross section σ_i is the measured cross section $\sigma_i^{(\text{expt})}$, trivially:

$$\sigma_i = \sigma_i^{(\text{expt})}. \tag{II.13}$$

If the population cross section of the i^{th} level cannot be determined from measurements, then Eq. II.5 is written down instead:

$$\sigma_i = \sum_k \alpha_{k,i}\sigma_k + \sigma_i^{(\text{side})} \tag{II.14}$$

where the summation over k covers all levels that decay directly (i.e. in one step) to the i^{th} level. Therefore, the matrix elements are given by

$$A_{i,j} = \begin{cases} 1 & \text{if } i = j \\ -\alpha_{j,i} & \text{if population } \sigma_i \text{ not measured} \\ 0 & \text{all other cases} \end{cases}. \tag{II.15}$$

Note the reversed order of indices between $A_{i,j}$ and $\alpha_{j,i}$. The right-hand-side vector elements are given by

$$b_i = \begin{cases} \sigma_i^{(\text{side})} & \text{if population } \sigma_i \text{ not measured} \\ \sigma_i^{(\text{expt})} & \text{otherwise} \end{cases}. \tag{II.16}$$

Thus for example, a straightforward application of Eqs. II.15 and II.16 to the simple level scheme in Fig. 1 will reproduce Eq. II.10 upon inversion of the matrix equation.

C Graphical Method

Once Eq. II.12 has been constructed using Eqs. II.15 and II.16, it must be solved for the ground state cross section σ_1. This is a tedious procedure which may produce cumbersome equations. In order to simplify this process, a graphical method is introduced to extract specific terms in the final expression for σ_1 without invoking the full machinery of matrix inversion. In the end, σ_1 is a sum of all the contributions to the ground state population, and in the formalism of this paper, these contributions have been divided into two types: i) calculated side feeding to a discrete level, and ii) measured population cross section of a discrete level. In either case, an initial discrete "starting" state in the level scheme is selected, and the initial cross section is tracked along a decay path to the ground state, provided it does not traverse a level whose population cross section can be deduced from the measured yield of a γ-ray depopulating it (otherwise, that level becomes the starting level). Each time the decay path breaks off into a new branch from a level, the de-excitation strength is scaled by the corresponding branching ratio. For the example in Fig. 1, there are five possible decay paths to the ground state that do not traverse a measured level, and therefore five terms in the sum that gives σ_1. These paths and the corresponding term in the sum are shown in Fig. 2. Adding all the contributions from these graphs produces

$$\begin{aligned}\sigma_1 &= \sigma_1^{(\mathrm{side})} + \alpha_{2,1}\sigma_2^{(\mathrm{side})} + \alpha_{2,1}\alpha_{3,2}\sigma_3^{(\mathrm{expt})} + \alpha_{4,1}\sigma_4^{(\mathrm{expt})} + \alpha_{4,2}\alpha_{2,1}\sigma_4^{(\mathrm{expt})} \\ &= \sigma_1^{(\mathrm{side})} + \sigma_2^{(\mathrm{side})} + \sigma_3^{(\mathrm{expt})} + \sigma_4^{(\mathrm{expt})},\end{aligned} \tag{II.17}$$

which is identical to Eq. II.10, obtained using the analytical matrix equation.

III. APPLICATION

The **sum** method can be applied to more realistic cases such as the $^{235}\mathrm{U}(n,2n)$ and $^{239}\mathrm{Pu}(n,2n)$ cross sections, recently investigated using partial γ-ray yields measured with the GEANIE spectrometer at LANSCE/WNR [3–5]. An estimate of the channel cross section for these reactions is deduced here using the **sum** method, and contrasted with the cross section obtained by the "**ratio**" method [5, 6], an alternate approach discussed in appendix A. The results are compared with independently-measured [7, 8] or evaluated [9] channel cross sections.

A Application: the $^{235}\mathrm{U}(n,2n)$ cross section

1 Experimental data

A partial level scheme for ^{234}U is displayed in Fig. 3. The transition arrows shown correspond to γ rays for which a yield was either directly measured [3] (solid arrows) or deduced (dotted arrows) from the measured yield of another γ ray from the same level using known branching ratios. The set of non-coincident γ rays displayed in Fig. 3 was chosen from all the observed transitions because it includes the $6_1^+ \rightarrow 4_1^+$ γ ray, the strongest and most reliably-measured transition. Several of the γ rays shown have nearly degenerate energies, which complicates the $^{235}\mathrm{U}(n,2n)$ cross-section estimate based on these data. The yield extracted for unresolved γ-ray energies represents the sum of the individual yields, while the matrix formulation of the **sum** method in Eqs. II.15 and II.16 seemingly requires individual transition cross sections, rather than their sum. The expedient solution is to discard those experimental levels for which an individual population cross section cannot be unambiguously extracted. This extreme approach reduces the amount of experimental information input to the **sum** method thereby increasing reliance on the model calculation. In fact, a case-by-case examination of the degenerate γ rays for the selection of levels in Fig. 3 reveals a more benign solution:

2 The E_γ = 880/880-keV degeneracy

An 880-keV transition appears twice in the level scheme: in the decay of the 3_2^- state at $E_x = 1023.8$ keV to the 4_1^+ level at $E_x = 143.4$ keV, and in the transition from the 4_3^+ level at $E_x = 1023.7$ keV to the 4_1^+ level at $E_x = 143.4$ keV. Using the graphical method described in section II C, it is possible to write all the contributions to the ground-state population from the $E_x = 1023.7$-keV and 1023.8-keV levels:

$$\begin{aligned}&\alpha_{2_1^+\to 0_1^+}\alpha_{4_1^+\to 2_1^+}\alpha_{3_2^-\to 4_1^+}\sigma^{(\mathrm{expt})}_{3_2^-} + \alpha_{2_1^+\to 0_1^+}\alpha_{4_1^+\to 2_1^+}\alpha_{4_3^+\to 4_1^+}\sigma^{(\mathrm{expt})}_{4_3^+}\\ &= \alpha_{2_1^+\to 0_1^+}\alpha_{4_1^+\to 2_1^+}\underbrace{\left[\alpha_{3_2^-\to 4_1^+}\sigma^{(\mathrm{expt})}_{3_2^-} + \alpha_{4_3^+\to 4_1^+}\sigma^{(\mathrm{expt})}_{4_3^+}\right]}_{\equiv\sigma^{(\mathrm{expt})}_{\mathrm{sum}}}\end{aligned} \tag{III.1}$$

where the level spin/parity/index J_i^π is used to label the levels. The quantity $\sigma^{(\mathrm{expt})}_{\mathrm{sum}}$ in the square brackets is the one measured in the experiment, rather than the individual transition cross sections $\sigma_{3_2^-\to 4_1^+} \equiv \alpha_{3_2^-\to 4_1^+}\sigma^{(\mathrm{expt})}_{3_2^-}$ and $\sigma_{4_3^+\to 4_1^+} \equiv \alpha_{4_3^+\to 4_1^+}\sigma^{(\mathrm{expt})}_{4_3^+}$. Fortunately, these individual cross sections are irrelevant, since only their sum ($\sigma^{(\mathrm{expt})}_{\mathrm{sum}}$) appears in the expression for the ground-state population cross section $\sigma_{0_1^+}$ (Eq. III.1). Therefore, in order to use the matrix formalism, it is always possible to write

$$\begin{aligned}\alpha_{3_2^-\to 4_1^+}\sigma^{(\mathrm{expt})}_{3_2^-} &\equiv \alpha_a\sigma^{(\mathrm{expt})}_{\mathrm{sum}}\\ \alpha_{4_3^+\to 4_1^+}\sigma^{(\mathrm{expt})}_{4_3^+} &\equiv \alpha_b\sigma^{(\mathrm{expt})}_{\mathrm{sum}},\end{aligned} \tag{III.2}$$

for any two number α_a and α_b satisfying the condition

$$\alpha_a + \alpha_b = 1. \tag{III.3}$$

In other words, it does not matter how the transition cross sections are divided up between the 3_2^- and 4_3^+ levels, it only matters that their combined contributions add up to $\sigma^{(\mathrm{expt})}_{\mathrm{sum}}$. Thus, the individual population cross sections

$$\begin{aligned}\sigma^{(\mathrm{expt})}_{3_2^-} &= \frac{\alpha_a}{\alpha_{3_2^-\to 4_1^+}}\sigma^{(\mathrm{expt})}_{\mathrm{sum}}\\ \sigma^{(\mathrm{expt})}_{4_3^+} &= \frac{\alpha_b}{\alpha_{4_3^+\to 4_1^+}}\sigma^{(\mathrm{expt})}_{\mathrm{sum}}\end{aligned} \tag{III.4}$$

can be used in the right-hand-side vector in Eq. II.12. In the present calculation, the value $\alpha_a = \alpha_b = 1/2$ was used.

3 The E_γ = 946/948-keV degeneracy

Two distinct transitions with energies $E_\gamma = 946$ keV ($2_1^- \to 2_1^+$) and 948 keV ($5_1^+ \to 4_1^+$) cannot be separated in the experiment. Therefore, the quantity

$$\sigma^{(\mathrm{expt})}_{\mathrm{sum}} \equiv \sigma_{2_1^-\to 2_1^+} + \sigma_{5_1^+\to 4_1^+} = \alpha_{2_1^-\to 2_1^+}\sigma^{(\mathrm{expt})}_{2_1^-} + \alpha_{5_1^+\to 4_1^+}\sigma^{(\mathrm{expt})}_{5_1^+} \tag{III.5}$$

is the one actually measured. The graphical method of section II C gives the contribution from the 2_1^- and 5_1^+ states:

$$\alpha_{2_1^+\to 0_1^+}\alpha_{2_1^-\to 2_1^+}\sigma^{(\mathrm{expt})}_{2_1^-} + \alpha_{2_1^+\to 0_1^+}\alpha_{4_1^+\to 2_1^+}\alpha_{5_1^+\to 4_1^+}\sigma^{(\mathrm{expt})}_{5_1^+}, \tag{III.6}$$

which cannot be factored a priori as in section III A 2. However, the $4_1^+ \to 2_1^+$ transition is the only branch from the 4_1^+ level, and therefore $\alpha_{4_1^+\to 2_1^+} = 1$. With this substitution, Eq. III.6 can be rewritten as

$$\begin{aligned}&\alpha_{2_1^+\to 0_1^+}\left[\alpha_{2_1^-\to 2_1^+}\sigma^{(\mathrm{expt})}_{2_1^-} + \alpha_{5_1^+\to 4_1^+}\sigma^{(\mathrm{expt})}_{5_1^+}\right]\\ &= \alpha_{2_1^+\to 0_1^+}\sigma^{(\mathrm{expt})}_{\mathrm{sum}},\end{aligned} \tag{III.7}$$

and once again, the individual cross sections

$$\begin{aligned}\sigma^{(\mathrm{expt})}_{2^-_1} &= \frac{\alpha_a}{\alpha_{2^-_1\to 2^+_1}}\sigma^{(\mathrm{expt})}_{\mathrm{sum}}\\ \sigma^{(\mathrm{expt})}_{5^+_1} &= \frac{\alpha_b}{\alpha_{5^+_1\to 4^+_1}}\sigma^{(\mathrm{expt})}_{\mathrm{sum}}\end{aligned} \tag{III.8}$$

can be used in Eq. II.12 using any two numbers α_a and α_b that satisfy Eq. III.3. In practice, $\alpha_a = \alpha_b = 1/2$ was used.

4 The E_γ = 925/926/927-keV degeneracy

The E_γ = 925, 926, and 927-keV transitions from the E_x = 968.6 (3^+_1), 1069.3 (4^-_1), and 926.7 keV (2^+_3) levels respectively are also degenerate within experimental resolution. The sum of all three transitions is measured:

$$\begin{aligned}\sigma^{(\mathrm{expt})}_{\mathrm{sum}} &\equiv \sigma_{3^+_1\to 2^+_1} + \sigma_{4^-_1\to 4^+_1} + \sigma_{2^+_3\to 0^+_1}\\ &= \alpha_{3^+_1\to 2^+_1}\sigma^{(\mathrm{expt})}_{3^+_1} + \alpha_{4^-_1\to 4^+_1}\sigma^{(\mathrm{expt})}_{4^-_1} + \alpha_{2^+_3\to 0^+_1}\sigma^{(\mathrm{expt})}_{2^+_3}.\end{aligned} \tag{III.9}$$

On the other hand, the graphical method yields the contribution

$$\begin{aligned}&\alpha_{2^+_1\to 0^+_1}\alpha_{3^+_1\to 2^+_1}\sigma^{(\mathrm{expt})}_{3^+_1} + \alpha_{2^+_1\to 0^+_1}\alpha_{4^+_1\to 2^+_1}\alpha_{4^-_1\to 4^+_1}\sigma^{(\mathrm{expt})}_{4^-_1} + \alpha_{2^+_3\to 0^+_1}\sigma^{(\mathrm{expt})}_{2^+_3}\\ &+\alpha_{2^+_1\to 0^+_1}\alpha_{2^+_3\to 2^+_1}\sigma^{(\mathrm{expt})}_{2^+_3} + \alpha_{2^+_1\to 0^+_1}\alpha_{4^+_1\to 2^+_1}\alpha_{2^+_3\to 4^+_1}\sigma^{(\mathrm{expt})}_{2^+_3}\end{aligned} \tag{III.10}$$

to the $\sigma_{0^+_1}$ cross section from the three parent levels. Using the substitution $\alpha_{4^+_1\to 2^+_1} = 1$, the first three term in Eq. III.10 could be factored into $\alpha_{2^+_1\to 0^+_1}\sigma^{(\mathrm{expt})}_{\mathrm{sum}}$. However, this still leaves the last two terms in Eq. III.10 which involve $\sigma^{(\mathrm{expt})}_{2^+_3}$. This situation differs from the cases discussed in sections III A 2 and III A 3 because one of the levels, the 2^+_3 state at E_x = 926.7 keV, decays by more than one transition, all of which are included in the cross-section calculation but not in $\sigma^{(\mathrm{expt})}_{\mathrm{sum}}$. Fortunately, the yield for one of those γ rays, the E_γ = 883-keV $2^+_3 \to 2^+_1$ has been measured. As a result, the $\sigma^{(\mathrm{expt})}_{2^+_3}$ population cross section can be independently determined, and the problem can be reduced from that of a threefold to a twofold degeneracy. In practice, the sum

$$\begin{aligned}\sigma'^{(\mathrm{expt})}_{\mathrm{sum}} &\equiv \alpha_{3^+_1\to 2^+_1}\sigma^{(\mathrm{expt})}_{3^+_1} + \alpha_{4^-_1\to 4^+_1}\sigma^{(\mathrm{expt})}_{4^-_1}\\ &= \sigma^{(\mathrm{expt})}_{\mathrm{sum}} - \alpha_{2^+_3\to 0^+_1}\sigma^{(\mathrm{expt})}_{2^+_3}\end{aligned} \tag{III.11}$$

can be entirely determined from experimental data. Elements of the right-hand-side vector in Eq. II.12 can now be determined by the usual stratagem:

$$\begin{aligned}\sigma^{(\mathrm{expt})}_{3^+_1} &= \frac{\alpha_a}{\alpha_{3^+_1\to 2^+_1}}\sigma'^{(\mathrm{expt})}_{\mathrm{sum}}\\ \sigma^{(\mathrm{expt})}_{4^-_1} &= \frac{\alpha_b}{\alpha_{4^-_1\to 4^+_1}}\sigma'^{(\mathrm{expt})}_{\mathrm{sum}}\end{aligned} \tag{III.12}$$

where α_a and α_b are chosen to satisfy Eq. III.3. In this case as well, $\alpha_a = \alpha_b = 1/2$ was used.

B Calculation

The experimental data for ^{235}U$(n,2n)$ were combined with two versions of calculated cross sections, labeled **GNASH98** [10] and **GNASH00a** [11], obtained using the Hauser-Feshbach code GNASH. The latter calculation incorporates improvements based in part on GEANIE γ-ray data for the ^{235}U$(n,2n\gamma)$ reaction.[1] Comparison of $(n,2n)$ cross-section estimates based on the two GNASH calculations provides a sensitivity tests to some of the details of the model. The branching ratios in both GNASH predictions were adjusted from their values in the original calculation to include internal conversion effects. In the application of the **sum** method, only statistical uncertainties in the γ-ray data, and uncertainties in branching ratios used to extract level-population cross sections were included. The resulting cross sections are plotted in Fig. 4 and should be compared with the **ratio** method results in Fig. 5. (See Appendix A for a description of the **ratio** method). In Fig. 4, we see that using either the **GNASH98** or **GNASH00a** calculation, the **sum** method produces a higher cross section than the values measured by Frehaut *et al.* [7] in the E_n = 6–8 MeV range. For E_n = 8–11 MeV, the **sum** method agrees with the Frehaut values, and above 11 MeV, the Frehaut points have large error bars and are not reliable. Near threshold, the excitation-function shape is different in the **ratio** and **sum** methods. In the **ratio** method, the behavior near threshold can be affected by an artifact of the technique, as both numerator and denominator in the calculated partial-to-total ratio $S_{\rm obs}^{\rm (calc)}/\sigma_R^{\rm (calc)}$ used in the method approach zero. The **sum** method is well-behaved near threshold, and for this reason it is preferable to the **ratio** method. Away from threshold, it is impossible to know which methods yields the answer closest to the physical cross section, although both techniques give nearly the same values (at any incident neutron energy above E_n = 7 MeV, results from the two methods using the **GNASH00a** calculation differ by less than 4%).

Finally, it is worth noting that neither the **ratio** nor the **sum** method are model-independent. However, the **GNASH98** and **GNASH00a** calculated $(n,2n)$ cross sections in Fig. 4 differ by less that 11%, and likewise the $(n,2n)$ cross sections deduced by the **sum** method differ by less than 10% over the energy range above threshold. A model-independent lower limit on the $(n,2n)$ cross section can be obtained by setting $\sigma_i^{\rm (side)} = 0$ in Eq. II.16, and is shown in Fig. 6. This lower limit can be compared to the Frehaut data to quantify the fraction of the estimated $(n,2n)$ cross section contributed by the model calculation (e.g., $\approx$ 40% at E_n = 9.8 MeV). The **sum** method based on the **GNASH00a** calculation in Fig. 4 gives the preferred estimate of the ^{235}U$(n,2n)$ cross section because it incorporates the best available model calculation, and is well-behaved near threshold.

C Application: the ^{239}Pu$(n,2n)$ cross section

The ^{239}Pu$(n,2n)$ cross section is interesting as a diagnostic tool. The cross section has recently been deduced from γ-ray data using the **ratio** method [5]. In this section, the $(n,2n)$ cross section is obtained using the **sum** method. As with the ^{235}U$(n,2n)$ cross section discussed above, the ^{239}Pu case is discussed here to show a realistic application of the **sum** method; therefore only pertinent details are presented. Fig. 7 shows individual transition cross sections for γ rays used in the **sum** method compared to the most recent GNASH calculation, **GNASH00b** [12].[2] [3] Many of the measured γ-ray yields shown in Fig. 7 are underestimated by the calculation, while two of the strongest yields, for the 157-keV $6_1^+ \rightarrow 4_1^+$ transition and the 617-keV $3_1^- \rightarrow 2_1^+/5_1^- \rightarrow 4_1^+$ doublet, are closely matched. Only statistical uncertainties in the γ-ray data, and uncertainties in branching ratios used to extract level-population cross sections were included in the **sum**-method calculation. The final deduced cross sections, using both **ratio** or **sum** methods, are shown in Fig. 8 and compared to the data measured by Lougheed *et al.* [8] and an evaluation [9] based on the Lougheed *et al.* data and the **ratio**-method result. Below E_n = 8 MeV (near threshold), the **sum** and **ratio** methods agree because the **GNASH00b** calculation was optimized to better reproduce the GEANIE data. In the E_n = 8–14 MeV range, the **sum**-method prediction is lower than the **ratio**-method cross section by less than 12%. Above E_n = 14 MeV, the two methods give cross-section predictions that are consistent within uncertainties. Both **sum**- and **ratio**-method results are significantly closer to the Lougheed *et al.* measurements near 14 MeV [8, 9] than the $\sigma_{(n,2n)}$ value predicted by the **GNASH00b** calculation.

---

[1] The improvements consist of: i) turning off the built-in pre-equilibrium spin-transfer model, ii) using an extended set of levels in the discrete level scheme, and iii) using a modified value of the spin-cutoff parameter for the fission channel.

[2] The branching ratios in the **GNASH00b** prediction were adjusted from the original calculation to include internal conversion effects.

[3] The **GNASH00b** calculation was further corrected using a neutron-energy-dependent factor to account for small differences between the calculated and evaluated fission cross sections in the $(n,2n)$ cross section.

The **ratio** method produces a ^{239}Pu$(n,2n)$ cross section that is slightly closer to the Lougheed *et al.* points than the **sum**-method results and is insensitive to any variations in the reaction model that would change $S_{\rm obs}^{\rm (calc)}$ and $S_{\rm unobs}^{\rm (calc)}$ by the same multiplicative factor (see Eq. A2 in appendix A). In other words, the **ratio** method is robust under the assumption that the model correctly predicts the partial-to-total ratio $S_{\rm obs}^{\rm (calc)}/\sigma_R$ in Eq. A2. On the other hand, the **sum** method is generally better-behaved near threshold, and the error bars obtained in the threshold region are smaller than those calculated by the **ratio** method in this case. Unlike the ^{235}U$(n,2n)$ result in section III A, the model calculation for the ^{239}Pu$(n,2n)$ reaction reproduces the sum of measured partial cross sections, $S_{\rm obs}^{\rm (calc)}$, quite well near threshold. The **sum** and **ratio** methods are therefore in good agreement near threshold and there is no compelling reason to prefer the **sum** method over the **ratio** method. In fact, there is no way to decide a priori which method yields the estimate that is closest to the physical ^{239}Pu$(n,2n)$ cross section, and the prediction from either method must be evaluated to provide the best estimate of the $(n,2n)$ cross section.

IV. CONCLUSION

The **sum** method used to infer a reaction-channel cross section from measured partial γ-ray cross sections in the reaction-product nucleus has been discussed. In the method, complementary experimental and calculated cross-section contributions are added to estimate the reaction cross section. The cross sections derived in this way are well-behaved as a function of incident beam energy near threshold. A matrix representation of the method has been delineated to provide a rigorous framework within which γ-ray yields can be combined without the risk of double counting. This approach also provides a convenient separation between two phase of the reaction mechanism governed by distinct physics: side feeding of and transitions between discrete levels. A graphical approach is offered as an alternative to the cumbersome matrix algebra. The **sum** method has been applied to the realistic cases of the ^{235}U$(n,2n)$ and ^{239}Pu$(n,2n)$ cross sections, deduced from recently-measured γ-ray yields. Based on these examples, the **sum** method is preferred when calculated and measured partial γ-ray cross sections are not in good agreement near the reaction threshold. An alternate approach, the **ratio** method, is better suited in cases where it is known a priori that the ratio of the sum of observed partial γ rays to the $(n,2n)$ cross section is correctly predicted by the model.

V. ACKNOWLEDGMENTS

I wish to thank John Becker for a careful reading of this manuscript and countless useful suggestions. This work was performed under the auspices of the U.S. Department of Energy by the University of California, Lawrence Livermore National Laboratory under contract No. W-7405-Eng-48.

APPENDIX A: THE RATIO METHOD

It is instructive to compare the **sum**-method result in Eq. II.10 to an alternate scheme for combining measured and calculated cross sections: the **ratio** method. In the **ratio** method, the reaction cross section σ_R is estimated using the formula

$$\sigma_R = \frac{S_{\rm obs}^{\rm (expt)}}{S_{\rm obs}^{\rm (calc)}/\sigma_R^{\rm (calc)}}, \tag{A1}$$

where $S_{\rm obs}^{\rm (expt)}$ and $S_{\rm obs}^{\rm (calc)}$ are defined in section II A, and $\sigma_R^{\rm (calc)}$ is given by Eq. II.1. Equation A1 should be compared to the **sum**-method formula in Eq. II.2. Using Eq. II.1 the **ratio**-method definition in Eq. A1 can be rewritten as

$$\sigma_R = S_{\rm obs}^{\rm (expt)} + S_{\rm unobs}^{\rm (calc)} \times \left(\frac{S_{\rm obs}^{\rm (expt)}}{S_{\rm obs}^{\rm (calc)}} \right), \tag{A2}$$

which resembles the **sum**-method equation apart from the additional factor in parentheses. Comparing Eqs. II.2 and A2, it is clear that the two methods will yield the same value for the deduced reaction cross section if the measured and calculated sums of transition cross sections are the same (i.e., if $S_{\rm obs}^{\rm (expt)} = S_{\rm obs}^{\rm (calc)}$). Because of the additional

factor in Eq. A2, the **ratio** method may become ill-behaved near the reaction threshold, where both $S_{\rm obs}^{\rm (expt)}$ and $S_{\rm obs}^{\rm (calc)}$ approach zero (see, e.g., section III A). The **sum** method does not suffer from this limitation. On the other hand, if there is reason to believe that the ratio $S_{\rm obs}^{\rm (calc)}/\sigma_R^{\rm (calc)}$ is correctly predicted by the model, though the individual numerator and denominator may not be, the **ratio** method provides a more reliable estimate of the channel cross section than the **sum** method.

This last point is critical to the proper interpretation of either **sum**- or **ratio**-method results. In reaction-model calculations there may be good reasons to expect that the ratio $S_{\rm obs}^{\rm (calc)}/\sigma_R^{\rm (calc)}$ is well predicted by the model, but this is not necessarily the case. In fact, it is not difficult to construct a counter-example, where a comparison between measured and calculated γ-ray yields seems to indicate an overall scale factor discrepancy, but the application of the **ratio** method, which is designed to compensate for such a factor, yields a final answer farther from the physical reaction cross section than the **sum** method.

Consider the simple level scheme in Fig. 1 with branching ratios $\alpha_{4,1} = 0.80$ and $\alpha_{4,2} = 0.20$, and side-feeding cross sections from a "best" calculation listed in table I, along with the true (physical) side-feeding cross sections. The reaction cross section predicted by the calculation is given by (Eq. II.8)

$$\begin{aligned}\sigma_1^{\rm (best)} &= \sigma_1^{\rm (side)} + \sigma_2^{\rm (side)} + \sigma_3^{\rm (side)} + \sigma_4^{\rm (side)} \\ &= 50 + 150 + 52.7 + 47.3 = 300 \text{ mb},\end{aligned}$$

when in fact, the true reaction cross section is

$$\sigma_1^{\rm (true)} = 75 + 250 + 145 + 130 = 600 \text{ mb}.$$

Assume a perfect experiment is performed wherein the true partial γ-ray cross sections from levels 3 and 4 are measured:

$$\begin{aligned}\sigma_{3\rightarrow 2}^{\rm (expt)} &= \alpha_{3,2} \times \sigma_3^{\rm (side)} = 145 \text{ mb} \\ \sigma_{4\rightarrow 1}^{\rm (expt)} &= \alpha_{4,1} \times \sigma_4^{\rm (side)} = 104 \text{ mb},\end{aligned}$$

with the corresponding population cross sections $\sigma_3^{\rm (expt)} = 145$ mb and $\sigma_4^{\rm (expt)} = 130$ mb. The same partial cross sections are predicted by the best available calculation to be:

$$\begin{aligned}\sigma_{3\rightarrow 2}^{\rm (best)} &= \alpha_{3,2} \times \sigma_3^{\rm (side)} = 52.7 \text{ mb} \\ \sigma_{4\rightarrow 1}^{\rm (best)} &= \alpha_{4,1} \times \sigma_4^{\rm (side)} = 37.84 \text{ mb}.\end{aligned}$$

Thus the calculated partial cross sections for the $3 \rightarrow 2$ and $4 \rightarrow 1$ transitions are lower than the measured values by approximately the same factor of 2.75. Under these circumstances, it is tempting to invoke the **ratio** method when estimating the reaction cross section. Using Eq. II.11, we calculate

$$\begin{aligned}S_{\rm obs}^{\rm (expt)} &= 145 + 130 = 275 \text{ mb} \\ S_{\rm unobs}^{\rm (calc)} &= 300 \text{ mb} \\ S_{\rm obs}^{\rm (calc)} &= 52.7 + 47.3 = 100 \text{ mb},\end{aligned} \tag{A3}$$

and Eq. A1 then gives the **ratio**-method estimate

$$\begin{aligned}\sigma_1^{\rm (ratio)} &= \frac{275}{100/300} \\ &= 825 \text{ mb},\end{aligned}$$

which is 225 mb higher than the true value of 600 mb. Conversely, the **sum** method (Eq. II.10) gives

$$\begin{aligned} \sigma_1^{(\mathrm{sum})} &= 50 + 150 + 145 + 130 \\ &= 475 \text{ mb}, \end{aligned} \tag{A4}$$

which is only 125 mb lower than the actual value.

To be fair, it is possible to construct examples where the **ratio** method gives a better estimate of the reaction cross section than the **sum** method. In fact, neither method is guaranteed to produce a better estimate of the true reaction cross section. In light of this, the **sum** method should be understood as more than just an equation (Eq. II.2). The method also assumes implicitly that the model calculation of $S_{\mathrm{unobs}}^{(\mathrm{calc})}$ is correct and the data are accurate. The corresponding implicit assumption in the **ratio** method is that the quantity $S_{\mathrm{obs}}^{(\mathrm{calc})}/\sigma_R^{(\mathrm{calc})}$ is correctly predicted by the model.

REFERENCES

[1] Z. Sujkowski, D. Chmieleska, M. J. A. De Voigt, J. F. W. Jansen, and O. Scholten, Nucl. Phys. **A291**, 365 (1977).

[2] R. Broda, M. Ishihara, B. Herskind, H. Oeschler, and S. Ogaza, Nucl. Phys. **A284**, 356 (1975).

[3] W. Younes, J. A. Becker, L. A. Bernstein, P. E. Garrett, C. A. McGrath, D. P. McNabb, R. O. Nelson, M. Devlin, N. Fotiades, and G. D. Johns, *The* $^{235}U(n,2n\gamma)$ *Yrast Partial Gamma-Ray Cross Sections: A Report on the 1998 and 1999 GEANIE Data and Analysis Techniques*, Tech. Rep. UCRL-ID-140313, LLNL (2000).

[4] L. A. Bernstein, J. A. Becker, P. E. Garrett, K. Hauschild, C. A. McGrath, D. P. McNabb, W. Younes, M. Devlin, N. Fotiades, G. D. Johns, R. O. Nelson, and W. S. Wilburn, *Measurement of Several* $^{239}Pu(n,xn)$ *Partial* γ*-ray Cross Sections for* $x \leq 3$ *Using GEANIE at LANSCE/WNR*, Tech. Rep. UCRL-ID-140308, LLNL (2000).

[5] L. A. Bernstein, J. A. Becker, P. E. Garrett, W. Younes, D. P. McNabb, D. E. Archer, C. A. McGrath, H. Chen, W. E. Ormand, M. A. Stoyer, R. O. Nelson, M. B. Chadwick, *et al.*, Phys. Rev. C **65**, 021601 (2002).

[6] M. B. Chadwick and P. G. Young, *Calculated plutonium reactions for determining* $^{239}Pu(n,2n)^{238}Pu$, Tech. Rep. LA-UR-99-2885, LANL (1999).

[7] J. Frehaut, A. Bertin, and R. Bois, Nucl. Sci. Eng. **74**, 29 (1980).

[8] R. W. Lougheed *et al.* (2000), private communication.

[9] D. P. McNabb, J. D. Anderson, R. W. Bauer, J. A. Becker, F. Dietrich, P. Navratil, M. B. Chadwick, and P. G. Young, *Evaluation of the* $^{239}Pu(n,2n)$ *Integrated Cross Section*, Tech. Rep. UCRL-ID-143328, LLNL (2001).

[10] M. B. Chadwick and P. G. Young, *GNASH98 code output* (1999), private communication.

[11] M. B. Chadwick and P. G. Young, *GNASH00a code output* (2000), private communication.

[12] M. B. Chadwick and P. G. Young, *GNASH00b code output* (2000), private communication.

TABLES AND FIGURES

TABLE I: Numerical example of a "best" side-feeding calculation for the level scheme in Fig. 1 compared to true values of the cross sections. The numbers are chosen to illustrate potential limitations of the **ratio** method (see appendix A).

Cross section	Best value (mb)	True value (mb)
$\sigma_1^{(\mathrm{side})}$	50	75
$\sigma_2^{(\mathrm{side})}$	150	250
$\sigma_3^{(\mathrm{side})}$	52.7	145
$\sigma_4^{(\mathrm{side})}$	47.3	130

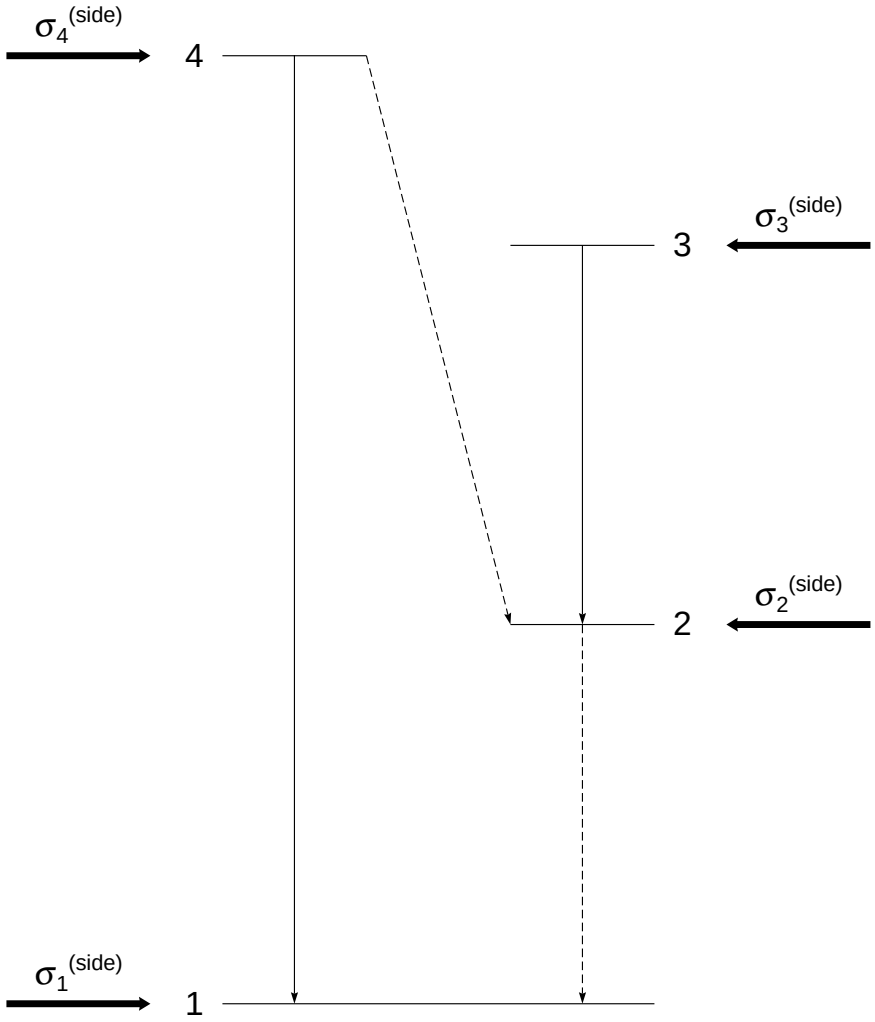

FIG. 1: Simple level scheme. The levels are labeled by integer indices. Solid downward arrows denote transitions for which a yield has been measured, and dashed arrows denote transitions for which yields were not measured. Side-feeding cross sections $\sigma_i^{(\mathrm{side})}$, calculated in a reaction-model code for each level i, are shown as horizontal arrows. It is assumed that all the branching ratios are known from experimental work.

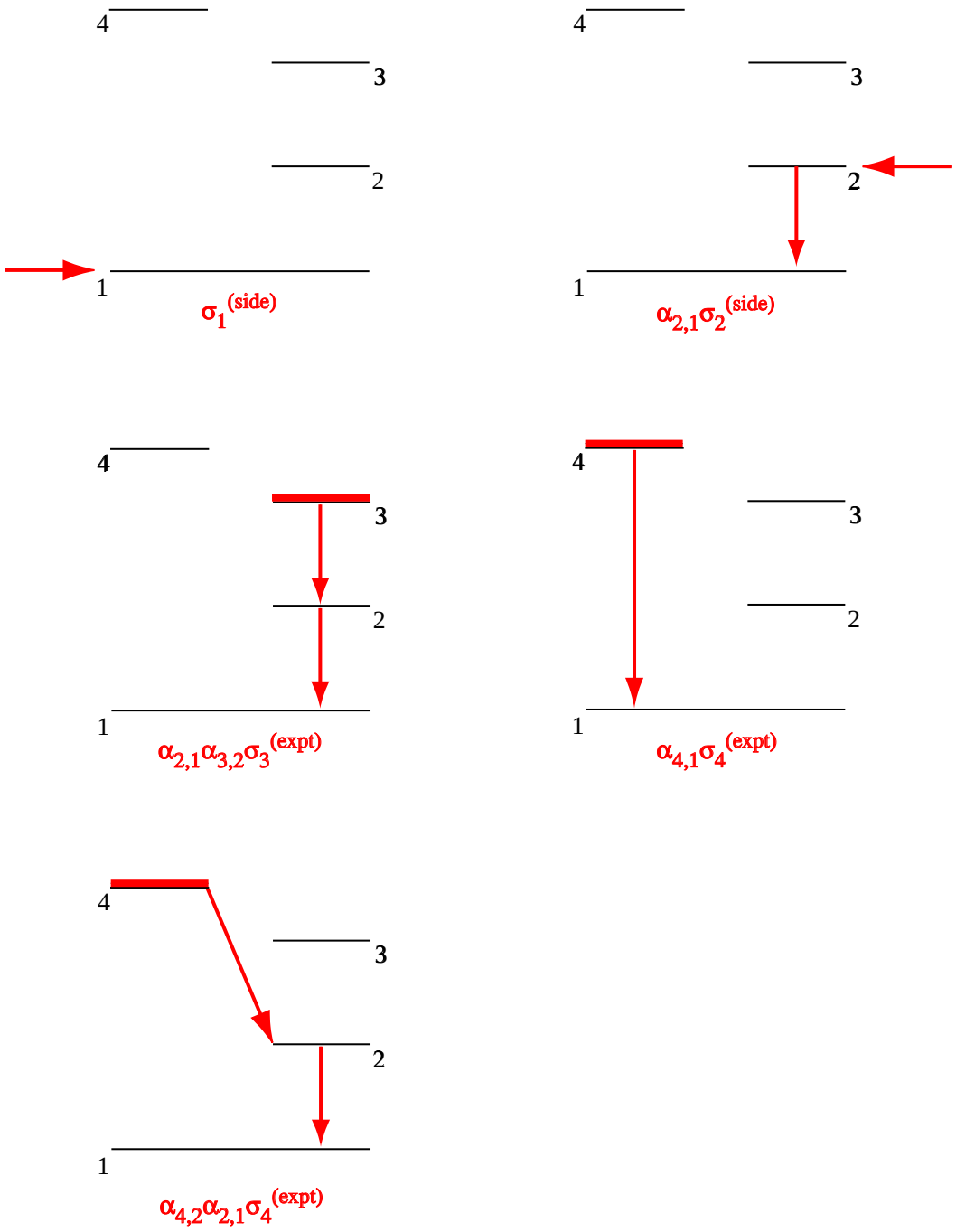

FIG. 2: Gamma-ray decay paths contributing to the total population of the ground state, for the level scheme in Fig. 1. Levels whose population cross section can be deduced from the yield of a γ ray depopulating it are highlighted in red. The decay path followed in each case is traced in red. Each of the five paths depicted is labeled by the corresponding term in the expression for the ground-state population cross section (Eq. II.17).

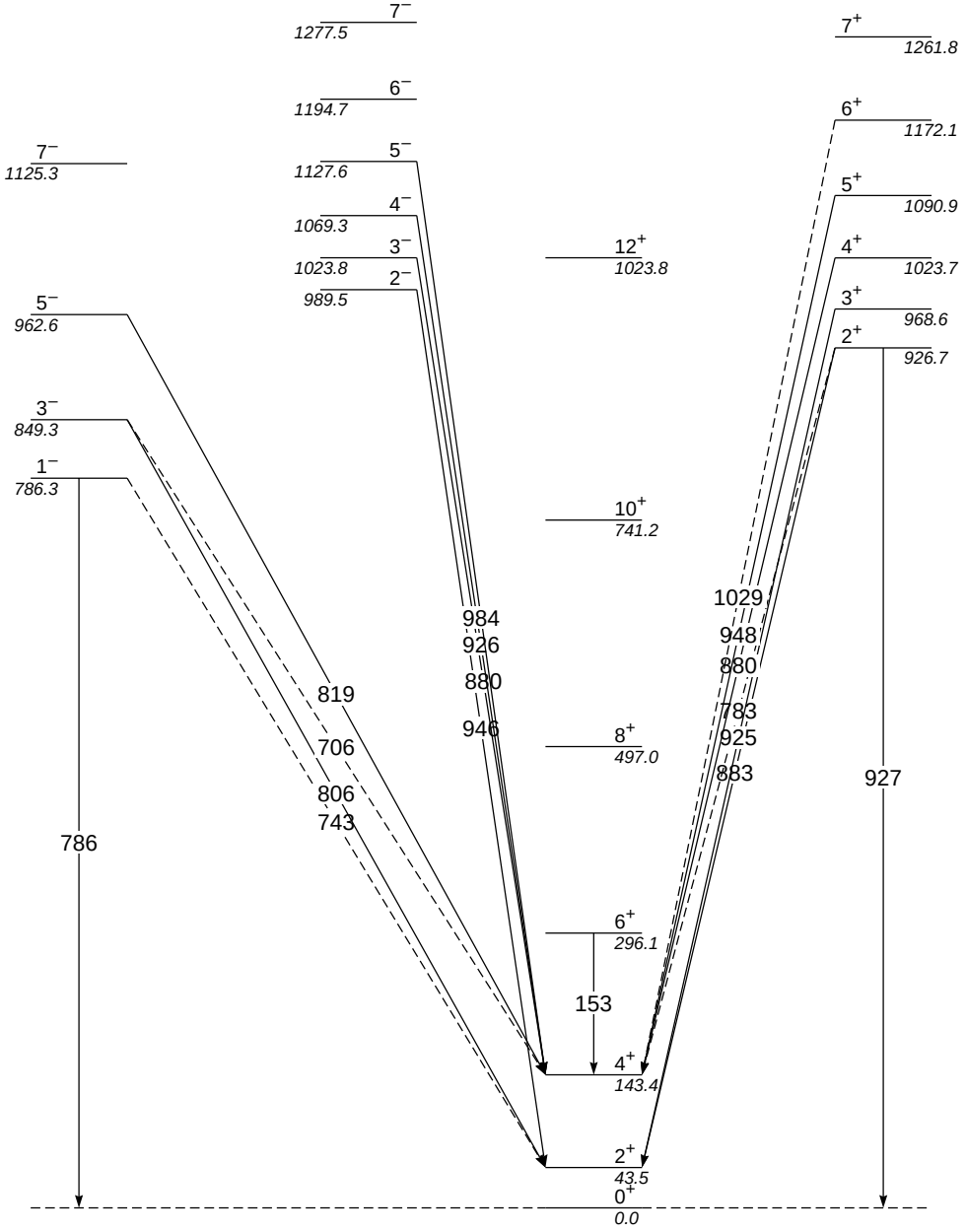

FIG. 3: Partial level scheme of ^{234}U showing the transitions used in the determination of the ^{235}U$(n, 2n)$ cross section (see section III A). Solid arrows denote transitions for which yields were measured, and dashed arrows imply that the corresponding transition could not be observed, but the yields were deduced using known branching ratios. Each transition arrow is labeled by the corresponding γ-ray energy.

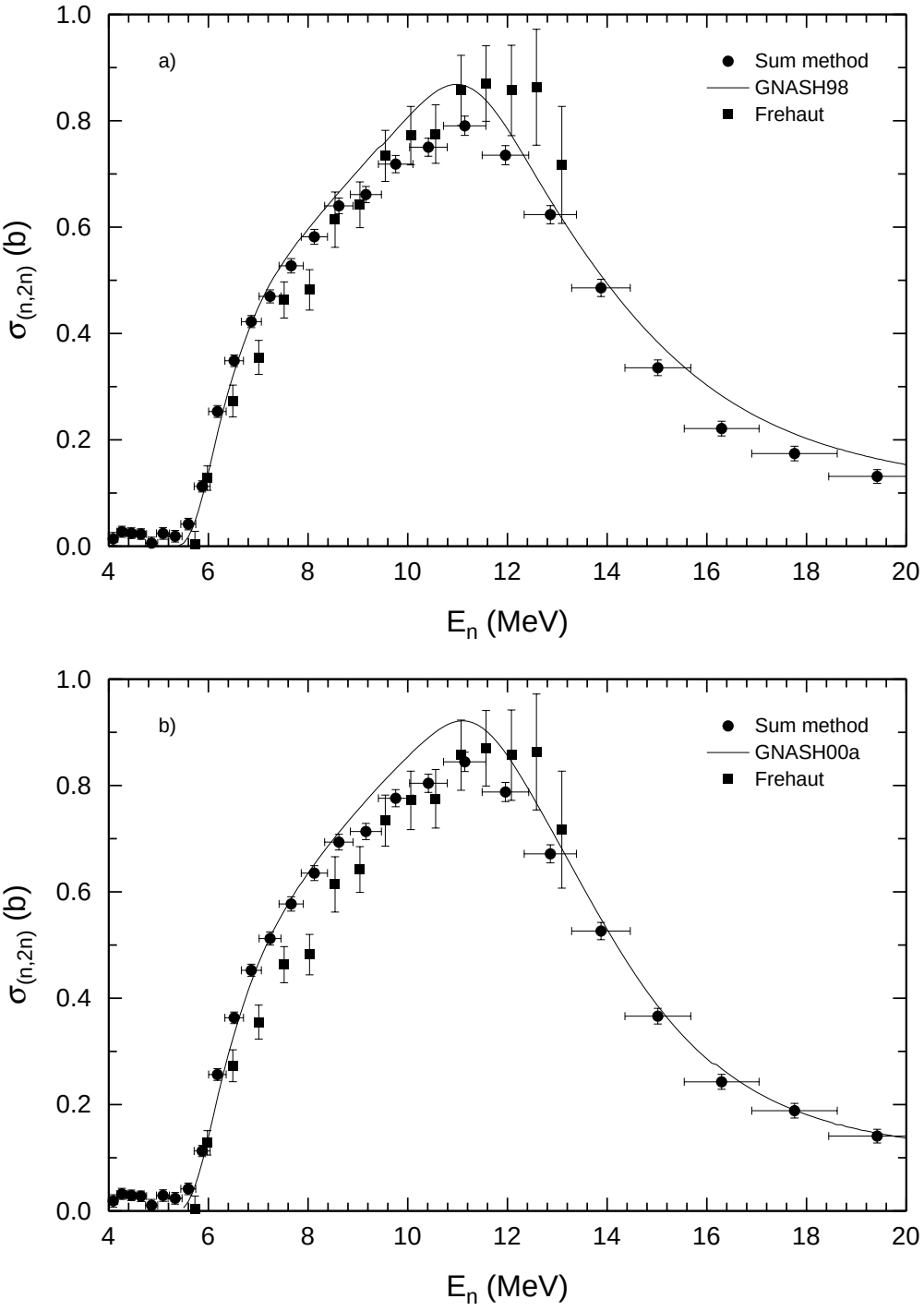

FIG. 4: **Sum**-method estimate of the ^{235}U$(n, 2n)$ cross section (solid circles) using measured γ-ray yields from experimental data [3], and supplemented by side-feeding cross sections from the a) **GNASH98** [10] and b) **GNASH00a** [11] calculations. Only statistical errors for the data and uncertainties in branching ratio used to deduce the measured level-population cross sections have been included. For comparison, the $(n, 2n)$ cross section from the GNASH calculation is shown as a solid line, and the Frehaut data [7] are plotted as solid squares in each case.

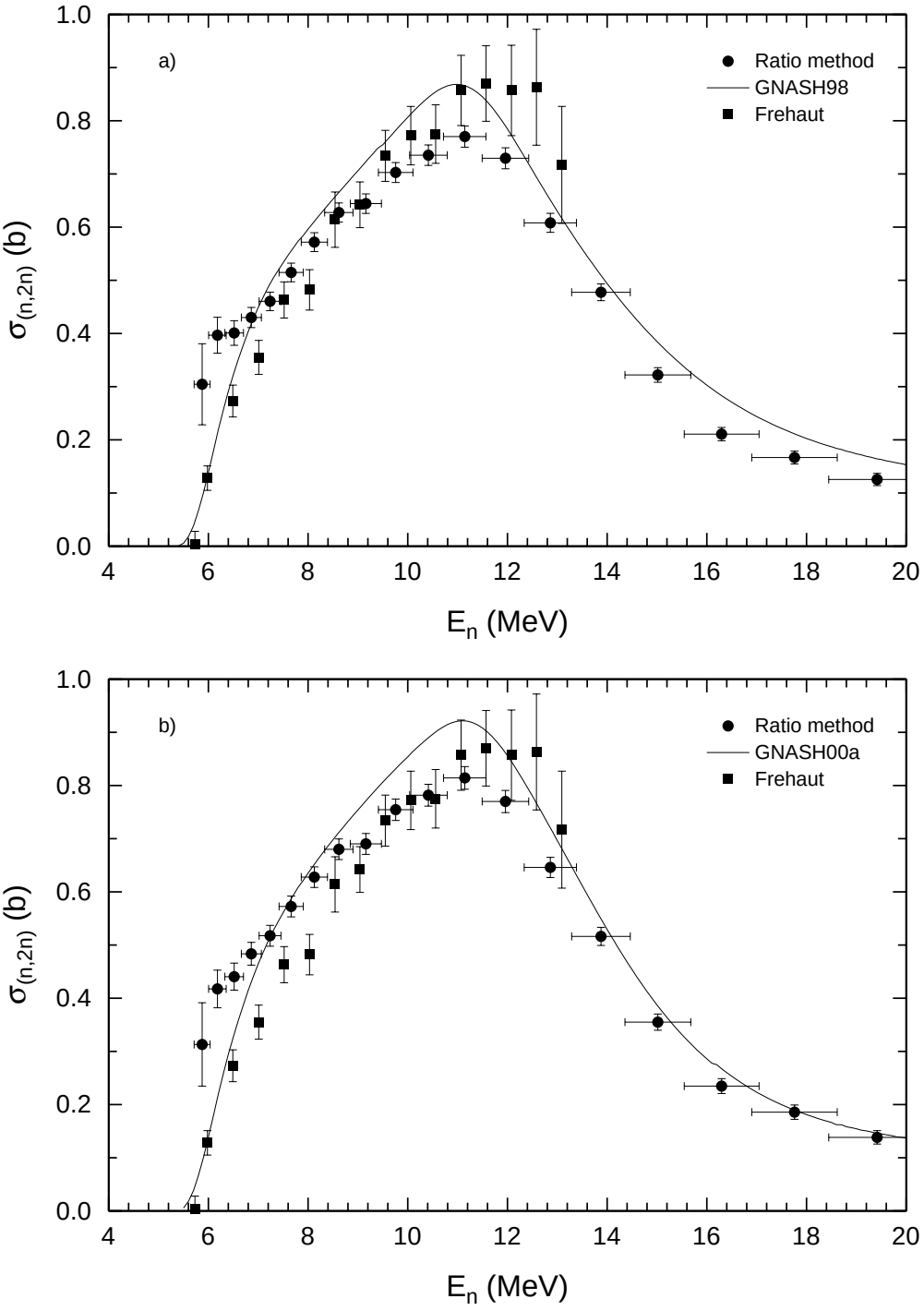

FIG. 5: **Ratio**-method estimate of the ^{235}U$(n,2n)$ cross section (solid circles) combining measured γ-ray yields from experimental data [3] with a) **GNASH98** [10] and b) **GNASH00a** [11] calculations. Only statistical errors have been considered for the data. For comparison, the $(n,2n)$ cross section from the calculation is shown as a solid line, and the Frehaut data [7] are plotted as solid squares. The cross section predicted by the **ratio** method near threshold differs significantly from that predicted by the **sum** method and plotted in Fig. 4. This discrepancy is interpreted as an artifact of the **ratio** method (see section III B).

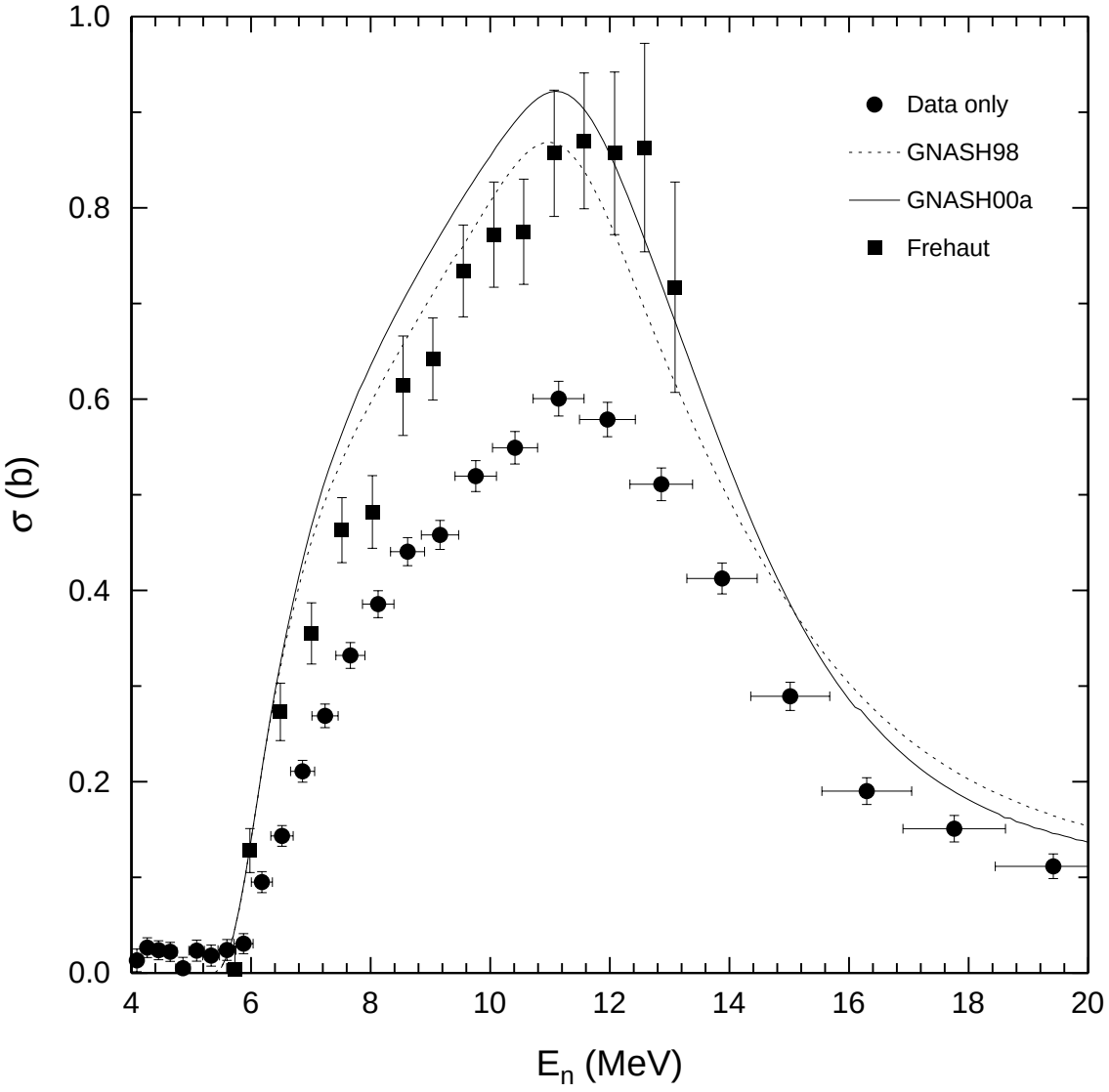

FIG. 6: Lower limit on the ^{235}U$(n,2n)$ cross section obtained by setting $\sigma_i^{(\mathrm{side})} = 0$ in Eq. II.16. Only statistical errors for the experimental data [3] and uncertainties on branching ratio used to deduce the measured level-population cross sections have been included. For comparison, the $(n,2n)$ cross section from the GNASH calculations are shown as dotted and solid lines [10, 11], and the Frehaut data [7] are plotted as solid squares. The difference between this lower limit and the Frehaut *et al.* data points gives the incremental cross section that the model calculation must supply to estimate the $(n,2n)$ cross section.

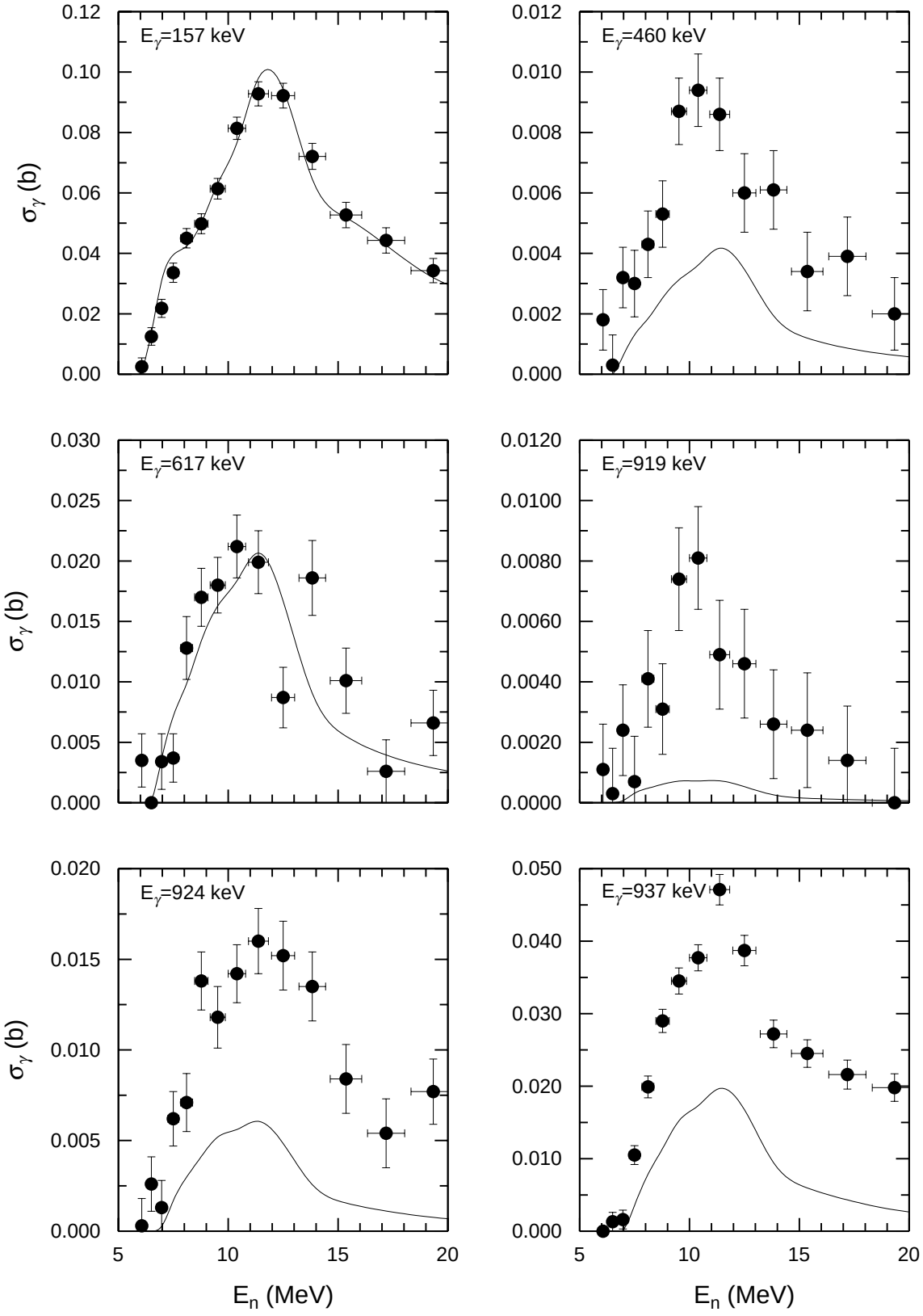

FIG. 7: Selection of partial γ-ray cross sections measured [5] in the ^{239}Pu$(n, 2n\gamma)$ reaction compared to **GNASH00b** calculations [12]. The γ rays are labeled by transition energy in each panel.

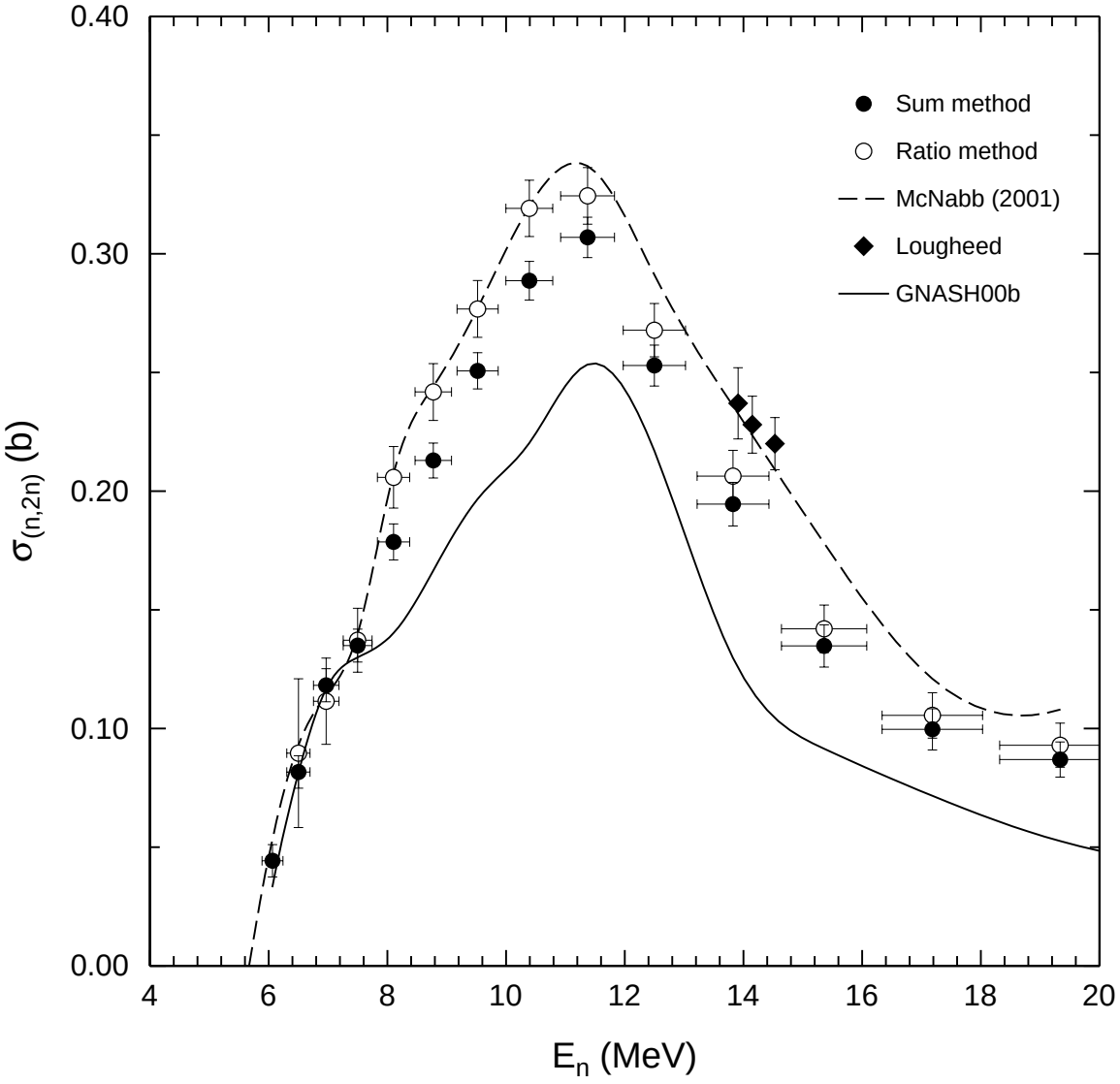

FIG. 8: The ^{239}Pu$(n, 2n)$ cross section determined using the **sum** and **ratio** methods with experimental data [5] and the **GNASH00b** calculation [12]. Data from Lougheed *et al.* [8, 9] and an evaluation by McNabb *et al.* [9], based on the **ratio**-method results and the Lougheed *et al.* data, are shown for comparison along with the **GNASH00b** prediction.